Journal of Mining and Environment (JME), Vol. 14, No. 1, 2023, 233-242

Shahrood University of Technology

Journal of Mining and Environment (JME)

Journal homepage: www.jme.shahroodut.ac.ir

Iranian Society of Mining Engineering (IRSME)

Investigation of Fracture Toughness of Shotcrete using Semi-Circular Bend Test and Notched Brazilian Disc test; Experimental Test and Numerical Approach

Mohammad Omidimanesh, Vahab Sarfarazi*, Nima Babanouri, and Amir Rezaei

Mining Engineering Department, Hamedan University of Technology, Hamedan, Iran

Article Info

Received 30 November 2022
Received in Revised form 6 December 2022
Accepted 15 December 2022
Published online 15 December 2022

DOI:10.22044/jme.2022.12465.2263

Keywords

Mode I fracture toughness
Discrete element method
Shotcrete

Abstract

This work presents the Semi-Circular Bend (SCB) test and Notched Brazilian Disc (NBD) test of shotcrete using experimental test and Particle Flow Code in two-dimensions (PFC2D) in order to determine a relation between mode I fracture toughness and the tensile strength of shotcrete. Firstly, the micro-parameters of flat joint model are calibrated using the results of shotcrete experimental test (uniaxial compressive strength and splitting tensile test). Secondly, numerical models with edge notch (SCB model) and internal notch (NBD model) with diameter of 150 mm are prepared. Notch lengths are 20 mm, 30 mm, and 40 mm. The tests are performed by the loading rate of 0.016 mm/s. Tensile strength of shotcrete is 3.25 MPa. The results obtained show that by using the flat joint model, it is possible to determine the crack growth path and crack initiation stress similar to the experimental one. Mode I fracture toughness is constant by increasing the notch length. Mode I fracture toughness and tensile strength of shotcrete can be related to each other by the equation, $\sigma t = 6.78 KIC$. The SCB test yields the lowest fracture toughness due to pure tensile stress distribution on failure surface.

1. Introduction

Shotcrete failure occurred from the propagation of one or more cracks, and thus could be considered as a fracture mechanics problem. It follows that the fracture toughness of shotcrete is important in theoretical studies and engineering applications related to shotcrete failure. Three methods for measuring shotcrete fracture toughness have been suggested by ISRM so far (Chen [1]; Huang [2]). Despite the standardization of the fracture toughness test, its use for shotcrete characterization and indexing purposes is not widespread—because of lengthy sample preparation time, premature failure of samples, and difficulties in obtaining consistent notch dimensions to the tolerances specified (Bearman [3]). Therefore, a simple method for determining fracture toughness of rock would be helpful. Shotcrete specimens in fracture toughness tests are typically core-based, and can be categorized into three groups based on their sampling shapes: cylindrical configurations (group I), disc configurations (group II), and half-disc configurations (group III). Group I includes the straight edge cracked round bar bend (SECRBB) method (Ouchterlony [4]) and two methods suggested by the International Society for Rock Mechanics (ISRM) for testing this group of materials: chevron bending (CB) and short rod (SR). These methods require access to long and intact rock cores (Cui et al. [5]). Group II, which is specimen geometry based on disk shapes, is the focus of many methods including the Brazilian disc (BD) method (Guo et al. [6]); the cracked straight through Brazilian disc (CSTBD) method (Awaji and Sato [7]1978, Atkinson et al. [8], Aliha et al. [9-11]); the double-edge cracked Brazilian disc (DECBD) method (Chen et al. [12]); the flattened Brazilian disc (FBD) method (Wang and Xing [13], Keles and Tutluoglu [14]); the hollow centre

* Corresponding author: Sarfarazi@hut.ac.ir (V. Sarfarazi)

cracked disc (HCCD) method (Amrollahi et al. [15]); the holed-cracked flattened Brazilian disc (HCFBD) method (Tang et al. [16]); the holed-flattened Brazilian disc (HFBD) method (Yang et al. [17]); the modified ring (MR) method (Thiercelin and Roegiers [18], Thiercelin [19], Tutluoglu and Keles [20]); the radial cracked rig method (Shiryaev and Kotkis [21]); and the ISRM-suggested cracked chevron notched Brazilian disc (CCNBD) method (Wang et al. [22], Iqbal and Mohanty [23], Dai et al. [24, 25]). The test methods conducted on half-disk geometries (Group III) include the notched semi-circular bend (NSCB) method (Dai and Xia [26], Kuruppu et al. [27]) and the cracked chevron notched semi-circular bend (CCNSCB) method (Kuruppu [28], Chang et al. [29], Dai et al. [30], Berto [31], Baek [32], Xu et al. [33]; Yaylaci [34-37]). These half-disc specimens have the advantage of simpler preparation and loading than the other two groups. Note that these semi-circular bending (SCB) type methods are also suitable for mixed mode fracture studies (Akbulut [38]). The notched semi-circular bend method has been widely used by the researchers, and was recently accepted as an ISRM-suggested method for measuring the mode I fracture toughness of rock (Kuruppu et al. [28] 2014a). The aim of this work is to determine a relation between mode I fracture toughness and the tensile strength of shotcrete using Semi-Circular Bend (SCB) test and Notched Brazilian Disc (NBD) test by experimental test and PFC2D. A comparison has been done between the SCB test result and the NBD test results. Also the applicability of flat joint model in PFC was determined.

1.1. NBD test

In a circular disk with a central vertical straight notch (β = 0) subjected to a diametrical compression load (Figure 1a), the tensile cracks propagate from the notch tip. In this condition, the following mathematical expression, proposed by Atkinson *et al*. [8], can be used for mode I fracture toughness calculation:

$$K_{IC} = \frac{P\sqrt{a}}{\sqrt{\pi}RB} N_I \quad (1)$$

$$N_I = 1 - 4sin^2\beta \times (1 - cos^2\beta)(a/R)^2 \quad (2)$$

1.2. SCB test

A SCB test to estimate macro-scale fracture toughness is performed using a semi-circular disc type with an artificial notch, as shown in Figure 1b. The details of this test are described in the ISRM-suggested methods published in Kuruppu [28]. The macro-scale mode-I fracture toughness (KIC) is represented using normalized stress intensity factor (YI), maximum load (Pmax), and dimension of specimen, as in Equation (3):

$$K_{IC} = \frac{P_{max}\sqrt{\pi a}}{2rt} Y_I \quad (3)$$

$$Y_I = -1.297 + 9.516\left(\frac{S}{r}\right) - \left(0.47 + 16.457\left(\frac{S}{r}\right)\right)\beta + \left(1.071 + 34.401(s/r)\right)\beta^2 \quad (4)$$

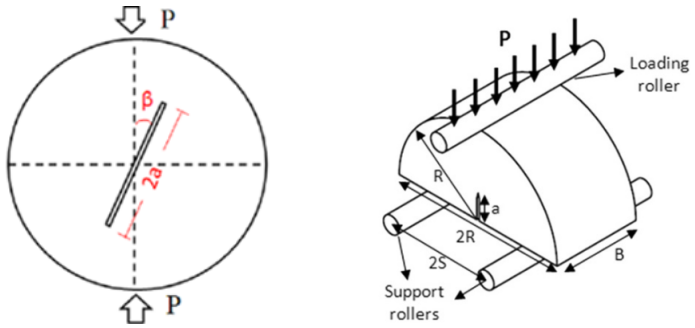

(a) (b)

Figure 1. a) Notched Brazilian disk specimen under diametrical compression (modified from Atkinson *et al.* [8], b) Geometry of SCB specimen.

2. Experimental Tests

The ingredients of shotcrete mixture are Portland cement, aggregate, water, and additives when necessary. In order to get the optimum strength and proper spraying ability of shotcrete mixture, correct proportions of ingredients and correct water/cement ratio are essential. It is known that the water/cement ratio of the shotcrete should be between 0.35-0.50 (M.G. Alexander and R. Heiyantuduwa, 2009). The required 7 days strength of shotcrete is between 25-30 MPa and 28 days strength is 35-40 MPa. Table 1 shows the ingredients of shotcrete mixture.

Table 1. Ingredients of shotcrete mixture.

Cement (g)	Water (mL)	Admixture (mL)	Aggregates (g)
180	90	1.8	1209

The mixing, casting, and curing of the specimens were carefully controlled to obtain reproducible specimens with precise properties. Mixing the material constituents was carried out with a blender. The mixed material was cast in a special mold for sampling rock-like discs. After removal of the shim, the specimen was stored in a laboratory environment at a controlled temperature of 20 ± 2 $^{\circ}$C for 10 days. It is important to note that consistency in mixing, casting, curing, and testing was required to obtain acceptable test results. The notch lengths in both of the NBD samples and SCB samples are 1 cm, 2 cm, and 3 cm. The opening of the notch was 1 mm. Figure 2 shows the experimental set up for the NBD test and the SCB test. Figure 3 shows failure pattern in the NBD samples and SCB samples. Totally, tensile crack was initiated from notch tip, and propagated parallel to the loading axis till coalescence with sample boundary.

(a) (b)

Figure 2. Experimental set up for a) NBD test and b) SCB test.

3. Particle Flow Code

Potyondy [39] developed the flat joint (FJ) model, while taking into consideration the polygonal particle grain structure (Figure 4). A pair of tightly connected locally flat notional surfaces that are centred at the contact point are used to represent the FJ contact. Each part has a face that acts as its imaginary surface and interacts with the faces of other parts. As a result, each facing grain looked to have a skirted, rounded, or spherical core. Discs or lines make up these faces (in 2D). A group of particles connected together by FJ connections is referred to as "flat-jointed material" (FJM). The line separating facing grains discretized into elements, and these elements may or may not be joined. Once FJ is positioned at a grain-to-grain contact, the torque as well as force at each element are then reset to zero and updated in line with the force-displacement law of bond as well as the relative movement of faces.

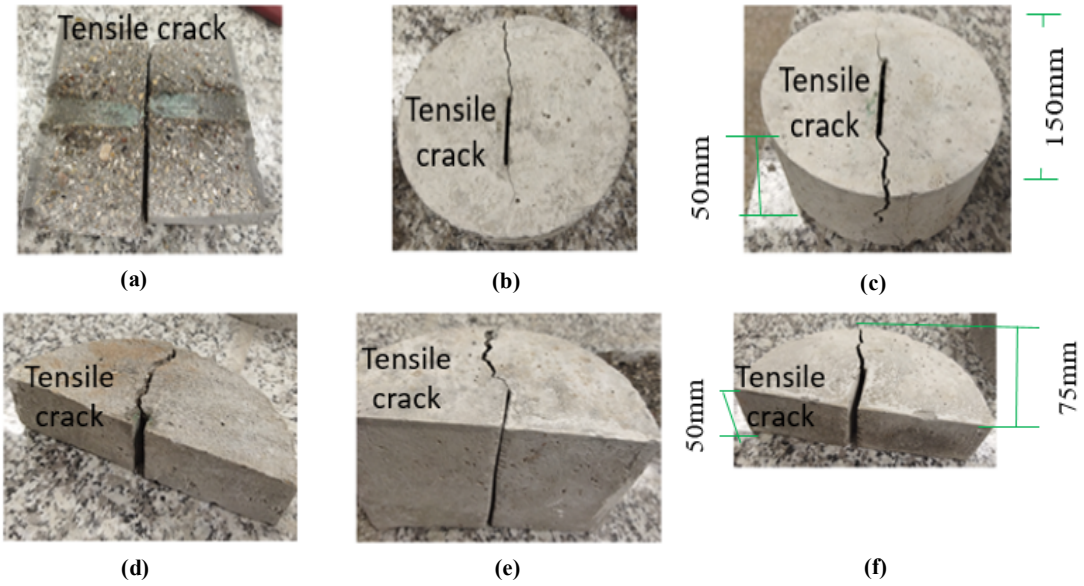

Figure 3. Failure pattern in NBD samples (a-c) and SCB samples (d-f).

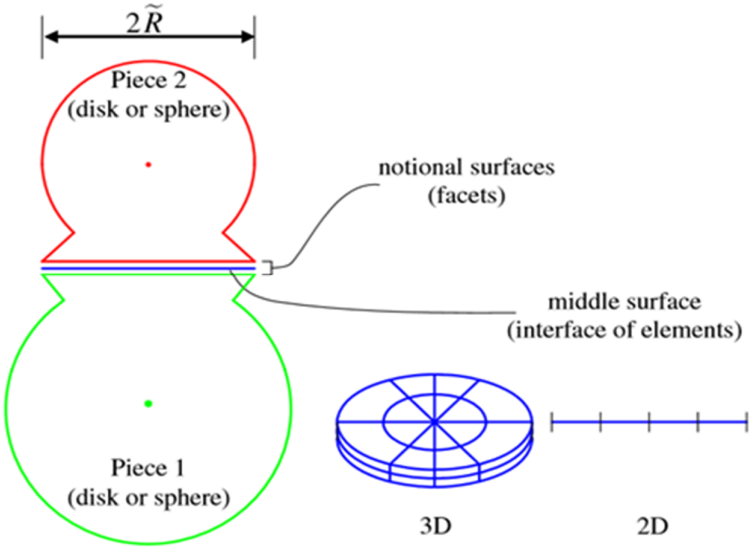

Figure 4. Flat-joint model (Potyondy [39]).

The shear force changed gradually but the normal force replaced immediately. The behaviour of the bonded element continues to be linear elastic as long as the strength does not go above its limit. The measurement of the maximum normal and shear stresses of element $\left(\sigma_{max}^{(e)}, \tau_{max}^{(e)}\right)$ based on the following:

$$\sigma_{max}^{(e)} = \frac{-\bar{F}_{(e)}^{n}}{A^{(e)}} \quad (5)$$

$$\tau_{max}^{(e)} = \frac{\bar{F}_{(e)}^{s}}{A^{(e)}} \quad (6)$$

where $A^{(e)}$ is the element area and $\bar{F}_{(e)}^{n}$ and $\bar{F}_{(e)}^{s}$ are normal and shear forces acting on the element, respectively. If the rotational resistance of the components and the torque contributions are minimal, a particular structure of facing grains may be used. The FJ components might be bonded or unbounded, as was already explained. The Coulomb criteria with the tension cut-off was used to determine the bonding element's strength. When the usual stress is larger than the tensile strength of the element $(\sigma_{max}^{(e)} > \sigma_b)$, elements rupture under tension, producing tensile cracks and changing their state from bonded to unbounded. The shear strength of element is specified by the bond cohesion c_b and the local friction angle $\emptyset_b$. When

the element's shear strength is less than the shear tension $\left[\tau_{max}^{(e)} > \tau_c = c_b - \bar{\sigma} tan\emptyset_b\right]$, the bond breaks during shear, changing its condition from bound to unbounded with lingering frictional strength. Unbounded elements have linear elastic behavior with frictional slip. According to the force-displacement legislation,

$$\bar{\sigma} = \begin{cases} 0 & \bar{g} \geq 0 \\ -k_n \bar{g} & \bar{g} < 0 \end{cases} \quad (7)$$

$$\bar{\tau} = \begin{cases} -\bar{\sigma} \tan \emptyset_r & \bar{\sigma} < 0 \\ 0 & \bar{\sigma} = 0 \end{cases} \quad (8)$$

where $\bar{g}$ is the element gap, $\tan \emptyset_r$ is the friction coefficient of unbonded element and $\emptyset_r$ is the residual friction angle. The dissociation of each bound element causes some damage to the FJ contact. When an FJ contact's relative displacement exceeds its diameter, the faces are disengaged, and if the particles re-engage, the force-displacement relationship is that of a linear contact model (Potyondy [40-41]).

3.1. PFC2D model preparation and calibration for shotcrete

The usual procedure for creating a PFC2D assembly is employed in this work for the construction of test models, and Potyondy [41] completely detail this procedure. Particle production, packing, isotropic stress installation (stress initialization), floating particle (floater), removal, and bond installation make up the procedure. The effects of gravity and the stress gradient caused by gravity on the macroscopic behaviour is minimal since the samples were tiny. Brazilian test calibration of particle characteristics and flat joint model was done. With the use of the micro-characteristics listed in Table 2 and standard calibration methods, a validated PFC particle assembly was produced. Figure 5 shows an experimental test results as well as a numerical simulation. The results showed a clear link between numerical simulation and experimentation. As demonstrated in Table 3, the derived specimen properties from the numerical models including the elastic modulus, Poisson's ratio, and UCS values, are likewise very similar to the actual values.

Table 2. Proper micro-properties.

Micro-characteristics of particles		Micro-characteristics of flat joints	
Model diameter (mm)	54	Gap ratio	0.5
Kn/ks	2	Ec (GPa)	6
Density (kg/m^3)	2500	Bonded friction	7
Smallest possible particle size (mm)	0.54	Strength in tension (MPa)	2.9
Maximum particle diameter (mm)	1.08	Tensile strength standard deviation (MPa)	0.29
Ec (GPa)	6	Cohesion (MPa)	10
Porosity	0.08	Cohesion standard deviation (MPa)	1
		Number of elements	2
		Kn/ks	2

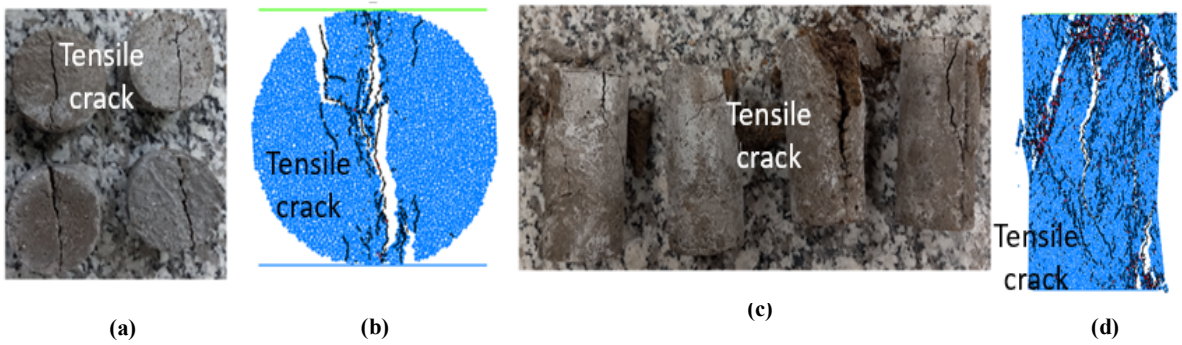

Figure 5. a) Brazilian experimental test, b) Brazilian numerical test, c) uniaxial experimental test, d) uniaxial numerical test.

Table 3. Comparison of macro-mechanical characteristics between model and experiments.

Mechanical characteristics	Experimental results	PFC2D Model results
Elastic modulus (GPa)	18	18
Poisson's ratio	0.	0.2
UCS (MPa)	35	35.5
Brazilian tensile strength (MPa)	3.25	3.3

3.2. NBD test and SCB test

The diameter of the NBD specimen and SCB specimen was identically taken into account in the equivalent physical test in the numerical modelling (i.e. 100 mm). The notch lengths in both of the NBD samples and SCB samples are 1 cm, 2 cm, and 3 cm. The opening of the notch was 1 mm. The tests were performed by loading rate of 0.016 mm/s. By measuring the reaction forces on the upper wall in Figure 6, the crack initiation force was calculated. Crack development in tests is seen in Figure 6. Tensile cracks are shown as black lines, whereas shear cracks are shown as red lines. The tensile fracture begins at the joint points and spreads parallel to the loading axis until coalescing at the sample edge. The similarity between Figures 6 and 3 demonstrates that both the experimental samples and the computational models experienced the same failure pattern.

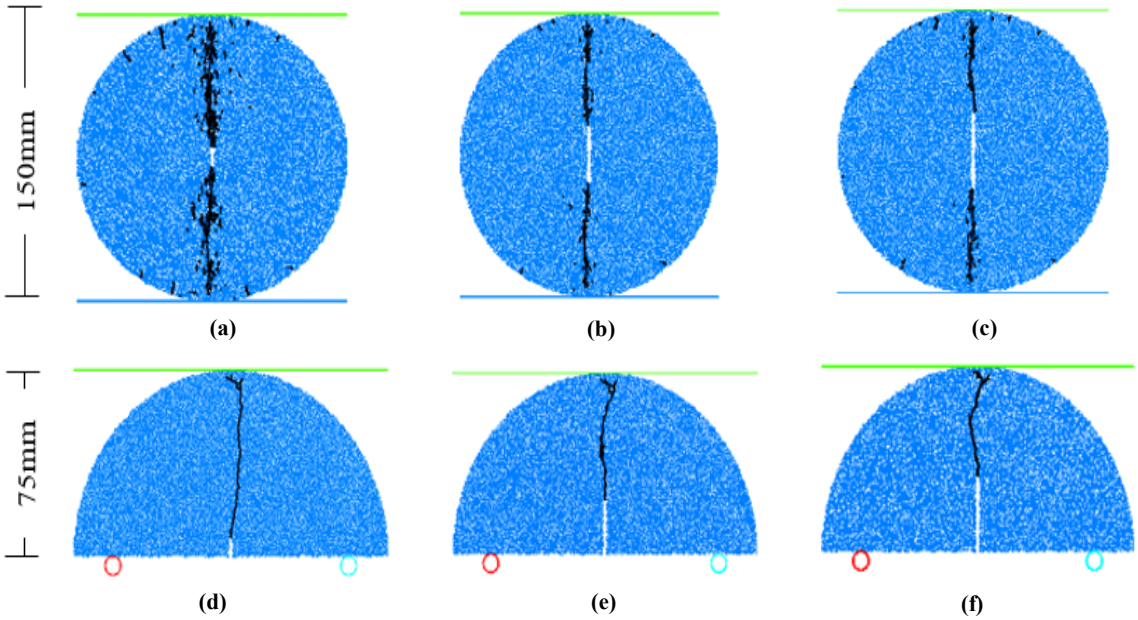

Figure 6. Failure pattern in NBD samples (a-c) and SCB samples (d-f).

3.3. Comparison between fracture toughness in numerical models

Table 4 and Table 5 show a comparison between the fracture toughness for the NBD and SCB tests in experimental test and numerical simulation, respectively. Also Table 4 and Table 5 show the tensile strength of intact shotcrete. The results show that Mode I fracture toughness was constant by increasing the notch length. The SCB test yields the lowest fracture toughness due to pure tensile stress distribution on failure surface. Mode I fracture toughness and tensile strength of shotcrete can be related to each other by the equation, σ_t = 6.78 KIC.

Table 4. A comparison between the experimental fracture toughness for NBD and SCB tests.

Test method	Notch length (cm)	Fracture toughness (MPa m½)	Tensile strength (MPa)
NBD	1	0.49	3.3
	2	0.48	3.3
	3	0.49	3.31
SCB	1	0.43	3.26
	2	0.44	3.24
	3	0.44	3.25

Table 5. A comparison between the numerical fracture toughness for NBD and SCB tests.

Test method	Notch length (cm)	Fracture toughness (MPa m½)	Tensile strength (MPa)
NBD	1	0.49	3.3
	2	0.5	3.3
	3	0.49	3.3
SCB	1	0.43	3.3
	2	0.44	3.3
	3	0.44	3.3

4. Conclusions

The results show that:

- By using flat joint model, it is possible to determine the crack growth path and crack initiation stress similar to the experimental one.
- Mode I fracture toughness and tensile strength of shotcrete can be related to each other by the equation $\sigma_t = 6.78$ KIC.
- Advantages by SCB tests are: (1) the SCB test need less sample size compared with other tests, (2) less material is needed for sample preparation, (3) sample preparation is easy, and (4) the use of a simple conventional compression press controlled by displacement compared with complicate device in other tests.
- Experimentally, the measurement of fracture toughness of shotcrete is more complicated and more expensive than that of tensile strength. Therefore, the relation given here provides a helpful method for estimating the fracture toughness from the tensile strength value, which can be measured more easily. In order to investigate the reasons for the relation more deeply, a further theoretical and experimental study is necessary.

References

[1]. Chen, X., Li, W., and Li, H. (2009). Evaluation of fracture properties of epoxy asphalt mix- tures by SCB test. J. Southeast Univ. 25 (4): 527–530.

[2]. Huang, B., Li, G., and Mohammad, L.N. (2003). Analytical modeling and experimental study of tensile strength of asphalt concrete composite at low temperatures. Comput. Part B Eng. 34 (8): 705–714.

[3]. Bearman R.A. (1999). The use of the point load test for the rapid estimation of mode I fracture toughness. Int J Rock Mech Min Sci; 36:257–63.

[4]. Ouchterlony F. (1982) A review of fracture toughness testing of rocks. Solid Mech Arch 7:131–211.

[5]. Cui ZD, Liu D.A., An G.M., Sun B., Zhou M., and Cao F.Q. (2010). A comparison of two ISRM suggested chevron notched specimens for testing Mode-I rock fracture toughness. Int J rock Mech Min Sci 47:871–876.

[6]. Guo H., Aziz N.I., and Schmidt L.C. (1993). Rock fracture toughness determination by the Brazilian test. Eng Geol. 33 (3): 177–188.

[7]. Awaji. H., and Sato. S. (1978). Combined mode fracture toughness measurement by disk test. J Eng Mater Technol. 100 (2):175–182.

[8]. Atkinson. C., Smelser. R.E., and Sanchez. J. (1982). Combined mode fracture via the cracked Brazilian disk test. Int J Fract. 18 (4): 279–291.

[9]. Aliha. M.R.M., Ayatollahi. M.R., Smith. D.J., and Pavier. M.J. (2010). Geometry and size effects on fracture trajectory in a limestone rock under mixed mode loading. Eng Fract Mech. 77 (11): 2200–2212.

[10]. Aliha. M.R.M., Ayatollahi. M.R., and Akbardoost. J. (2012). Typical upper bound-lower bound mixed mode fracture resistance envelopes for rock material. Rock Mech Rock Eng. 45 (1): 65–74.

[11]. Aliha. M.R.M., Sistaninia. M., Smith. D.J., Pavier. M.J., and Ayatollahi. M.R. (2012b) Geometry effects and statistical analysis of mode I fracture in guiting limestone. Int J Rock Mech Min Sci 51:128– 135.

[12]. Chen. C.H., Chen. C.S., and Wu. J.H. (2008) Fracture toughness analysis on cracked ring disks of

anisotropic rock. Rock Mech Rock Eng. 41 (4): 539–562.

[13]. Wang. Q.Z. and Xing. L. (1999) Determination of fracture toughness KIc by using the flattened Brazilian disc specimen for rocks. Eng Fract Mech 64 (2):193–201.

[14]. Keles. C., and Tutluoglu. L. (2011). Investigation of proper specimen geometry for mode I fracture toughness testing with flattened Brazilian disc method. Int J Fract. 169 (1):61–75.

[15]. Amrollahi. H., Baghbanan A., and Hashemolhosseini. H. (2011). Measuring fracture toughness of crystalline marbles under modes I and II and mixed mode I-II loading conditions using CCNBD and HCCD specimens. Int J Rock Mech Min Sci 48(7):1123–1134.

[16]. Tang. T., Bazˇ ant. Z.P., Yang S., and Zollinger D. (1996). Variable-notch one-size test method for fracture energy and process zone length. Eng Fract Mech. 55 (3):383–404.

[17]. Yang. S., Tang. T.X., Zollinger. D., and Gurjar A. (1997). Splitting tension tests to determine rock fracture parameters by peak-load method. Adv Cem Based Mater 5:18–28.

[18]. Thiercelin. M., and Roegiers. J.C. (1986). Fracture toughness determination with the modified ring test. In: Proceedings of the International Symposium on Engineering in Complex Rock Formations, Beijing, China, pp 1–8.

[19]. Thiercelin. M. (1989). Fracture toughness and hydraulic fracturing. Int J Rock Mech Min Sci Geomech Abstr 26:177–183.

[20]. Tutluoglu. L., and Keles. C. (2011). Mode I fracture toughness determination with straight notched disk bending method. Int J Rock Mech Min Sci. 48. (8): 1248–1261.

[21]. Shiryaev. A.M., and Kotkis. A.M. (1982). Methods for determining fracture-toughness of brittle porous materials. Ind Lab. 48 (9): 917–918.

[22]. Wang. Q.Z., Jia. X.M., Kou. S.Q., Zhang. Z.X., and Lindqvist. P.A. (2003). More accurate stress intensity factor derived by finite element analysis for the ISRM suggested rock fracture toughness specimen-CCNBD. Int J Rock Mech Min Sci. 4 (2): 233–241.

[23]. Iqbal MJ and Mohanty B (2007). Experimental calibration of isrm suggested fracture toughness measurement techniques in selected brittle rocks. Rock Mech. Rock Eng. 40 (5): 453–475.

[24]. Dai. F., Chen. R., Iqbal. M.J., and Xia. K. (2010). Dynamic cracked chevron notched Brazilian disc method for measuring rock fracture parameters. Int J Rock Mech Min Sci. 47 (4): 606–613.

[25]. Dai. F., Chen. R., and Xia. K. (2010). A semi-circular bend technique for determining dynamic fracture toughness. Exp Mech. 50 (6): 783–791.

[26]. Dai. F., and Xia. K. (2013). Laboratory measurements of the rate dependence of the fracture toughness anisotropy of Barre granite. Int J Rock Mech Min Sci 60: 57–65.

[27]. Kuruppu, M.D. (2014a) ISRM-suggested method for determining the mode I static fracture toughness using semi-circular bend specimen. Rock Mech. Rock Eng. 47: 267–274.

[28]. Kuruppu M.D., Obara. Y., Ayatollahi. M.R., Chong. K.P., and Funatsu. T. (2014). ISRM-Suggested method for determining the mode I static fracture toughness using semi-circular bend specimen. Rock Mech Rock Eng. 47 (1): 267–274.

[29]. Chang. S.H., Lee. C.I., and Jeon. S. (2002). Measurement of rock fracture toughness under modes I and II and mixed-mode conditions by using disc-type specimens. Eng Geol. 66 (1): 79–97.

[30]. Dai. F., Wei. M.D., Xu. N.W., Ma. Y., and Yang. D.S. (2015) Numerical assessment of the progressive rock fracture mechanism of cracked chevron notched Brazilian disc specimens. Rock Mech Rock Eng. 48 (2):463–479.

[31]. Berto, F., Cendon, D.A., Lazzarin, P., Elices, M. (2013). Fracture behavior of notched round bars made of PMMA subjected to torsion at −60 ˚C. Eng. Fract. Mech. 102, 271–287.

[32]. Baek, S.H., Hong, J.P., Kim, S.U., Choi, J.S., and Kim, K.W. (2011). Evaluation of fracture toughness of semi-rigid asphalt concretes at low temperatures. Transp. Res. Rec. 2210, 30–36.

[33]. Xu. N.W., Dai. F., Wei. M.D., Xu. Y., and Zhao. T. (2015). Numerical observation of three dimensional wing-cracking of cracked chevron notched Brazilian disc rock specimen subjected to mixed mode loading. Rock Mech Rock Eng. 32(2):33-44.

[34]. Yaylaci. M., and Birinci. A. (2013). The receding contact problem of two elastic layers supported by two elastic quarter planes. Structural Engineering and Mechanics, 48(2): 241-255.

[35]. Yaylaci. M., Öner. E., and Birinci. A. (2014). Comparison between Analytical and ANSYS Calculations for a Receding

[36]. Yaylacı M and Avcar M (2020). Finite element modeling of contact between an elastic layer and two elastic quarter planes. Computers and Concrete, Vol. 26, No. 2 (2020) 107-114.

[37]. Yaylacı M, Terzi C, and Avcar M. (2019). Numerical analysis of the receding contact problem of two bonded layers resting on an elastic half plane. Structural Engineering and Mechanics, 72 (6).

[38]. Akbulut, H and Aslantas, K (2004). Finite element analysis of stress distribution on bitu- minous pavement and failure mechanism. Mater. Des. 26, 383–387.

[39]. Potyondy, D.O. (2012). A flat-jointed bonded-particle material for hard rock. Paper presented at the 46th U.S. Rock Mechanics/Geomechanics Symposium, Chicago, USA.

[40]. Potyondy, D.O. (2015). The bonded-particle model as a tool for rock mechanics research and application: Current trends and future directions. Geosystem Engineering, 18(1): 1–28.

[41]. Potyondy, D.O. (2017). Simulating perforation damage with a flat-jointed bonded-particle material. Paper presented at the 51st US Rock Mechanics/Geomechanics Symposium, San Francisco, California, USA.

مطالعه چقرمگی شکست شاتکریت با استفاده از آزمایش‌های خمش نیم دایره‌ای و دیسک برزیلی شیاردار: تست آزمایشگاهی و شبیه سازی عددی

محمد امیدی منش، وهاب سرفرازی*، نیما بابانوری و امیر رضایی

بخش مهندسی معدن، دانشگاه صنعتی همدان، همدان، ایران

ارسال ۲۰۲۲/۱۱/۳۰، پذیرش ۲۰۲۲/۱۲/۱۵

* نویسنده مسئول مکاتبات: sarfarazi@hut.ac.ir

چکیده:

در این مقاله چقرمگی شکست شاتکریت با استفاده از تست‌های خمش نیم دایره‌ای و دیسک برزیلی شیاردار تعیین شد. همچنین رابطه بین مقاومت کششی شاتکریت و چقرمگی کششی مود I مطالعه شد. این مهم با استفاده از تست‌های آزمایشگاهی و شبیه سازی عددی انجام شد. درابتدا با استفاده از نتایج آزمایشگاهی (تست کشش برزیلی و تست تک محوره)، مقادیر میکروپارامترهای مدل درزه مسطح کالیبره شد. سپس آزمایش‌های خمش نیم دایره‌ای و دیسک برزیلی شیاردار توسط نرم افزار PFC شبیه سازی شد. قطر مدل ۱۵۰ میلیمتر و طول شکاف‌ها، ۱۰ ، ۲۰ و ۳۰ میلیمتر می‌باشد. نرخ بارگذاری ۰/۰۱۶ میلیمتر بر ثانیه است. مقاومت کششی شاتکریت ۳/۲۵ مگاپاسکال است. نتایج نشان می‌دهد که با استفاده از مدل درزه مسطح می‌توان تنش شروع ترک و الگوی شکست مشابه با نمونه آزمایشگاهی بدست آورد. با افزایش طول درزه، چقرمگی شکست شاتکریت ثابت است. ارتباط بین چقرمگی شکست شاتکریت و مقاومت کششی برابر است با $K_{IC} = 6.78\ \sigma_t$. مقادیر چقرمگی شکست حاصل از آزمایش خمش نیم دایره ای کمتر از تست دیسک برزیلی شیاردار است.

کلمات کلیدی: چقرمگی شکست مود کششی، روش اجزا مجزا، شاتکریت.